

Raisins in a Hydrogen Pie: Ultrastable Cesium and Rubidium Polyhydrides

Di Zhou,* Dmitrii Semenok,* Michele Galasso, Frederico Gil Alabarse, Denis Sannikov, Ivan A. Troyan, Yuki Nakamoto, Katsuya Shimizu, and Artem R. Oganov*

A new method for synthesis of metal polyhydrides via high-pressure thermal decomposition of corresponding amidoboranes in diamond anvil cells is proposed. Within this approach, molecular semiconducting cesium (P4/nmm-CsH₇, P1-CsH_{15+x}) and rubidium (RbH_{9-x}) polyhydrides with a very high hydrogen content reaching 93 at.% are synthesized. Preservation of CsH₇ at near ambient conditions, confirmed both experimentally and theoretically, represents a significant advance in the stabilization of hydrogen-rich compounds. In addition, two crystalline modifications of RbH_{9-x} with pseudohexagonal and pseudotetragonal structures identified by synchrotron X-ray diffraction, and Raman measurements are synthesized. Both phases are stable at 8–10 GPa. This is an unprecedentedly low stabilization pressure for polyhydrides. These discoveries open up possibilities for modifying existing hydrogen storage materials to increase their efficiency.

1. Introduction

Stabilizing polyhydrides is crucial for developing hydrogen batteries and environmentally-friendly vehicles based on them.^[1] Preservation of a H-rich shell can be achieved by the local electric field of a metal atom in neutral and charged clusters such as ThH₅⁻,^[2] LaH₈^{-[3]} (Figure 1a,c), in organic complexes due to field of ligands (Figure 1b), and via applying external pressure to metal polyhydrides, for instance, YH₆^[4] and CeH₉₋₁₀^[5] (Figure 1d). Frankly speaking, metal polyhydrides could be perfect materials for hydrogen storage, but the synthesis of most of them requires ultrahigh pressure of millions of atmospheres. When pressure is reduced, polyhydrides usually decompose irreversibly.

However, there is an exception to this rule: molecular polyhydrides of alkali and alkaline earth elements are much more stable and require only tens of GPa for their synthesis.^[6,7] The aim of this paper is to examine this important exception.

In general, the synthesis and stabilization pressure of polyhydrides decreases with decreasing ionization potential and atomic radius of alkali metal atoms. At least four insulating lithium hydrides were synthesized by compression of LiH with hydrogen up to 130–182 GPa including theoretically predicted LiH₂ and LiH₆.^[16,17] The formation of sodium polyhydrides already requires significantly lower pressures. Compression of NaH and hydrogen to 40 GPa with consequent laser heating leads to the formation of NaH₃ and molecular NaH₇.^[18,19] The later phase contains H⁻, linear and bent H₃⁻, and H₂ units at the same time. Formation of KH₅ and RbH₉ under relatively low pressure was also discussed.^[20,21] Continuing this series, as far as we know, no experimental attempts have been made to synthesize Cs polyhydrides. Insufficient experimental research on Cs and Rb hydrides prompted us to take on this work. Moreover, Cs and Rb are especially convenient for studies under pressure since they are rather heavy elements and crystal structure of their hydrides can be easily determined using X-ray diffraction.

Cesium and rubidium are very active alkali metals, which, according to ab initio calculations, react with H₂ to form polyhydrides already at low pressures of 10–30 GPa.^[22] Theoretical crystal structural searches show that RbH, RbH₅, RbH₉, CsH, CsH₃, CsH₇, and CsH₉ are the most thermodynamically stable phases at high pressures.^[22–25] Great chemical reactivity of these metals,

D. Zhou, D. Semenok
Center for High Pressure Science & Technology Advanced Research
Bldg. #8E, ZPark, 10 Xibeiwang East Rd, Haidian District, Beijing 100193, China

E-mail: di.zhou@hpstar.ac.cn; dmitrii.semenok@hpstar.ac.cn

M. Galasso
Institute of Solid-State Physics
University of Latvia
8 Kengaraga str., Riga LV-1063, Latvia

F. G. Alabarse
Elettra Sincrotrone Trieste
Strada Statale 14 – km 163,5 in AREA Science Park, Basovizza, Trieste 34149, Italy

D. Sannikov, A. R. Oganov
Skolkovo Institute of Science and Technology
Bolshoy Boulevard 30, bld. 1, Moscow 121205, Russia
E-mail: a.oganov@skoltech.ru

I. A. Troyan
Shubnikov Institute of Crystallography
Kurchatov Complex of Crystallography and Photonics
NRC “Kurchatov Institute”
59 Leninsky Prospekt, Moscow 119333, Russia

Y. Nakamoto, K. Shimizu
KYOKUGEN
Graduate School of Engineering Science
Osaka University
Machikaneyamacho 1–3, Toyonaka, Osaka 560–8531, Japan

The ORCID identification number(s) for the author(s) of this article can be found under <https://doi.org/10.1002/aenm.202400077>

DOI: 10.1002/aenm.202400077

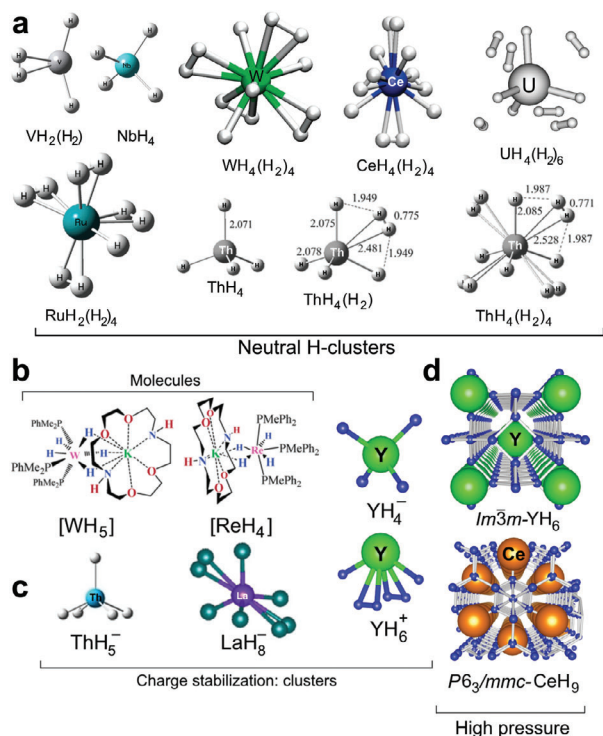


Figure 1. Examples of polyhydrides stabilization: a) in neutral clusters (gas phase),^[8–13] b) in complex organic compounds (solutions),^[14] c) in charged clusters (plasma),^[2,3] d) in 3D crystal structures of polyhydrides stabilized under high pressure.^[15]

low melting points of Cs and Rb, and high surface tension in the liquid state, seriously complicate study of the reactions of Cs and Rb with hydrogen. There is a popular method for the synthesis of polyhydrides in diamond anvil cells (DACs): the heating of metal precursors with ammonia borane (NH_3BH_3 , AB), which at high temperatures serves as a source of hydrogen. In fact, this method cannot be directly applied to Cs and Rb, since both of them react violently with NH_3BH_3 to form corresponding amidoboranes: CsAB and RbAB.^[26] Remarkably, these amidoboranes do not undergo further reactions with metallic Cs and Rb and can be used as both hydrogen and metal sources for high-pressure high-temperature synthesis of polyhydrides.

We propose a new approach to metal polyhydrides via the thermal decomposition of their amidoboranes in high-pressure DACs. The applicability of this method is illustrated by the examples of Cs and Rb polyhydrides. New CsH_7 , CsH_{15+x} , and two modifications of $\text{RbH}_{9,x}$ were synthesized at pressures of 10–40 GPa. The latter phases remain stable below 10 GPa, while CsH_7 can be decompressed to near-ambient pressure. These properties of cesium and rubidium polyhydrides open up the possibilities for modifying existing hydrogen storage materials to increase their efficiency.

2. Results

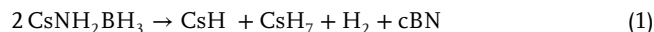
2.1. Synthesis of Cesium Polyhydrides: CsH_7 and CsH_{15+x}

Ammonia borane is a very convenient hydrogen source for synthesis of polyhydrides in DACs.^[15] Cs and Rb can easily react with

ammonia borane to form transparent salts called amidoboranes. We used two methods to synthesize them at ambient temperature and pressure in an argon glovebox: 1) solid-state mixing Cs or Rb with AB; 2) reaction of both metals with a saturated solution of ammonia borane in tetrahydrofuran (THF). The solid-state reaction is accompanied by excessive heating and yields the high-temperature (HT) crystal modifications of CsAB and RbAB, known from the literature.^[26] At the same time, the synthesis in THF solution leads to the low-temperature (LT) modifications of corresponding amidoboranes. Raman spectra of obtained amidoboranes can be found in Figures S9, S10, and S13 (Supporting Information). A more controlled reaction in THF solution is preferred.

As we observed, ultraviolet light (365 nm UV laser, Figures S6–S8, Supporting Information) cannot decompose amidoboranes of alkali metals with a release of hydrogen. Therefore we used infrared (1.04 μm) laser heating to promote their decomposition, and gold or Cs/Rb metal pieces as an IR light absorber. Amidoboranes CsAB and RbAB are transparent in the visible and near-IR range, which makes it impossible to continue laser heating as soon as the metal particle has reacted. To improve the heating process, we added a gold foil as an absorber of IR laser radiation. Follow-up Raman spectroscopy indicates that laser heating of CsAB and RbAB leads to their decomposition with the emission of hydrogen (Figures S11 and S15, Supporting Information).

In the first experiment, the Cs/LT-CsAB mixture was loaded into a Mao-type symmetric diamond anvil cell DAC X1 with an anvil culet diameter of 250 μm (Figure 2b). After increasing the pressure to 41 GPa, intense laser heating of the sample was carried out (see).^[27] As a result, almost all metallic Cs has reacted. After laser heating, we examined the resulting products using synchrotron X-ray diffraction (XRD) (Figure 2a). Comparison of XRD patterns (Figure 2a; Figure S33, Supporting Information) allowed us to detect characteristic diffraction pattern of cesium monohydride $Cmcm$ -CsH and diffraction peaks of the new compound, $P4/nmm$ -CsH₇, predicted as a part of evolutionary crystal structure search for stable Cs-H phases at 30 GPa (Figure 2e).^[28–30] In the following decompression experiment, CsH undergoes a phase transformation to $Pm\bar{3}m$ -CsH below 15 GPa, in accordance with the literature data.^[31] Experimental unit cell parameters of CsH and CsH₇ are given in Tables S2 and S3 (Supporting Information) The ratio of CsH and CsH₇ is close to 1:1 (Figure 2a), which speaks in favor of a disproportionation reaction:



Hydrogen produced in this reaction can in some cases be detected by Raman spectroscopy (Figures S11 and S15, Supporting Information), but in many other cases, it reacts with cesium or its hydrides forming new compounds, for example, CsH_{15+x} or CsH_3 , expected by analogy with NaH_3 .^[19] Cubic boron nitride (c-BN) is usually very poorly visible by X-ray diffraction due to small atomic scattering factors of B and N.

Tetragonal $P4/nmm$ -CsH₇ (Figure 1c) is a typical molecular-ionic polyhydride with a bandgap of ≈ 3.65 eV (HSE06) at 20 GPa (Figure S43, Supporting Information). Its unit cell contains one H^- ion and three hydrogen molecules ($d_{\text{HH}} = 0.81$ Å at 30 GPa). Presence of isolated hydride anions indicates a high potential

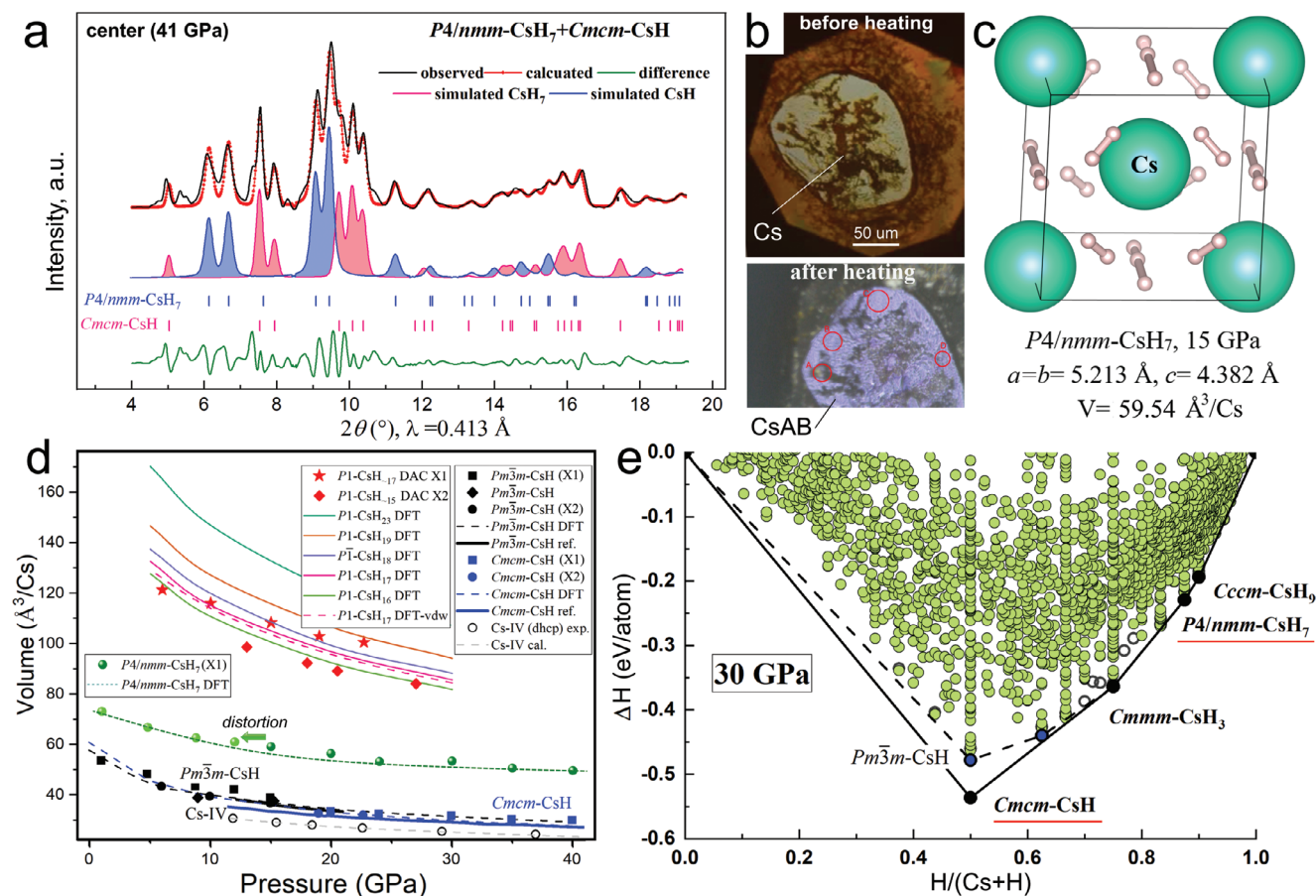


Figure 2. Synthesis of cesium hydride $P4/nmm\text{-CsH}_7$ at 41 GPa. When heated, cesium almost instantly reacts with hydrogen with the formation of transparent products. a) Experimental XRD pattern ($\lambda = 0.413 \text{ \AA}$, SPring-8) of reaction products after the laser heating of Cs/CsAB at 41 GPa. The black line is the experimental XRD pattern, the red one is the Le Bail refinement,^[32] the green one – is the difference. The blue shaded spectrum is the predicted XRD pattern of CsH_7 (Mercury 2021.2.0 code),^[33] and the pink one – is the same for $Cmcm\text{-CsH}$. b) Photographs of the Cs/CsAB sample before and after laser heating. c) Optimized unit cell of $P4/nmm\text{-CsH}_7$ at 15 GPa (PBE functional, VASP code).^[34–36] d) Experimental pressure vs. unit cell volume diagram for various studied cesium hydrides. Theoretical calculations are indicated by continuous lines and the “DFT” (density functional theory) marks. e) Thermodynamic convex hull of Cs-H system at 30 GPa and 0 K. The diagram is dominated by H-rich compounds. Stable phases are CsH, CsH_3 , CsH_7 , and CsH_9 (black circles).

ionic conductivity of the compound as observed for strontium,^[7] barium,^[37] and chlorine hydrides.^[38] Cs-sublattice in this compound is a deformed $Pm\bar{3}m$ structure, similar to the previously studied sodium polyhydride $Cc\text{-NaH}_7$.^[18] Surprisingly, during decompression of DAC X1, we found that the main series of XRD peaks of possibly distorted CsH_7 remains in the XRD pattern until the DAC is almost completely opened, indicating the unusual stability of cesium polyhydrides down to ≈ 1 GPa (Figures S34–S36, Supporting Information). Comparison with the theoretically predicted equation of state $V(P)$ (Figure 1d), shows that despite possible structural distortion, CsH_7 does not lose a lot of hydrogen at low pressures. Ab initio calculations confirm that $P4/nmm\text{-CsH}_7$ is thermodynamically stable down to 5 GPa at zero temperature (0 K). Additionally, harmonic phonon spectra indicate that CsH_7 remains dynamically stable even at ambient pressure (Figures S44–S47, Supporting Information). However, quantum molecular dynamics study within 10 ns at 300 K and atmospheric pressure indicates distortion of the tetragonal structure of CsH_7 , observed experimentally below 8 GPa, as

well as migration of hydrogen with a diffusion coefficient of $D_H \approx 3 \cdot 10^{-8} \text{ cm}^2 \text{ s}^{-1}$ (Figure S59, Supporting Information).

This first experiment demonstrated that cesium hydrides, CsH and CsH_7 , can be obtained as the main products from Cs/CsAB mixture via laser heating. However, it may happen that not all CsAB decomposes. This likely situation could lead to mixing and misinterpretation of the diffraction peaks from the cesium polyhydrides CsH_x and the residual amidoborane CsAB. Surprisingly, a separate experiment shows that compressed CsAB undergoes rapid and irreversible amorphization above 10 GPa (Figure S31, Supporting Information). Therefore, residual CsAB has no effect on the X-ray diffraction patterns of cesium polyhydrides. This fact greatly simplifies the synthesis and identification of Cs polyhydrides in the proposed approach.

In the second experiment (DAC X2), we investigated a mixture of cesium amidoborane and pieces of gold foil (Au/LT-CsAB) heated under pressure of 22 GPa. X-ray diffraction patterns of the synthesis products were studied at the *Elettra* synchrotron radiation facility, Xpress beamline (Trieste, Italy), and are shown

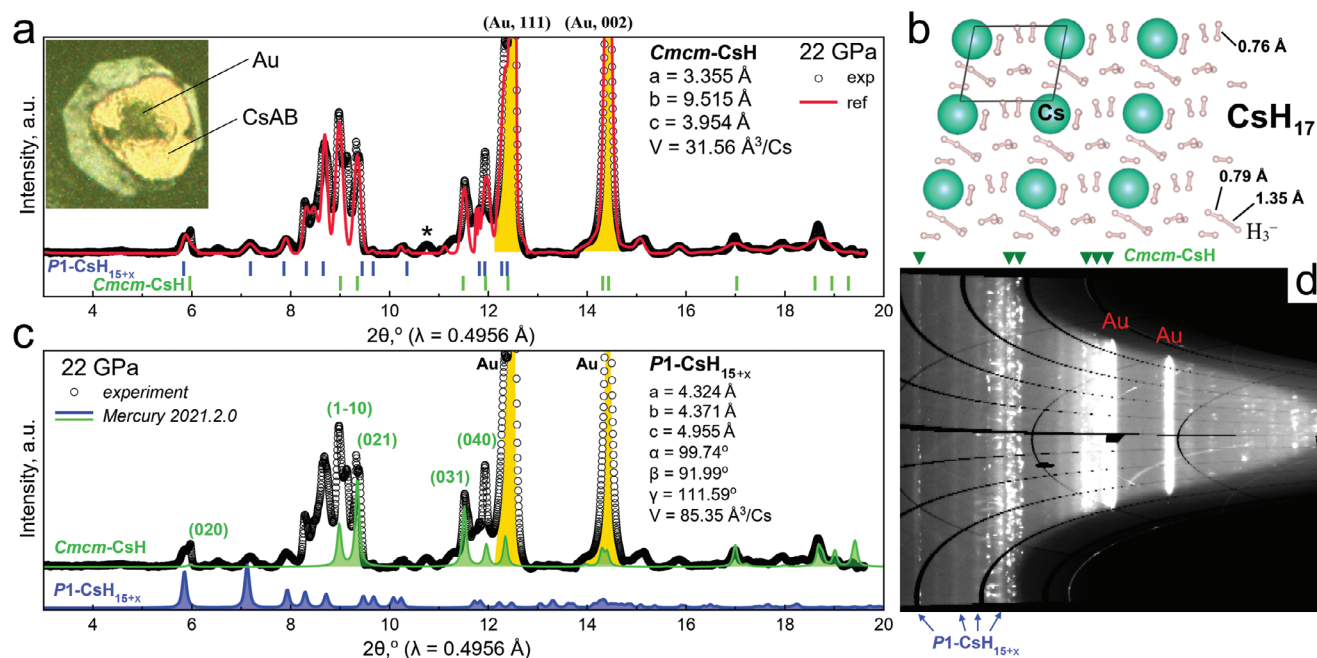


Figure 3. Formation of cesium polyhydride $P1\text{-CsH}_{15+x}$ from CsAB/Au below 27 GPa in DAC X2. a) Powder X-ray diffraction pattern of the reaction products in the vicinity of a gold target (black curve, $\lambda = 0.4956 \text{ \AA}$, Elettra). The black line is the experimental XRD pattern, the red line is the Le Bail refinement of the unit cell parameters of CsH_{15+x} , $Cmc\text{-CsH}$, and gold ("Au"). Diffraction peaks of gold are indicated in yellow. Inset: photo of DAC's chamber at 22 GPa. b) Optimized structure of CsH_{17} at 20 GPa (PBE functional, VASP code).^[34-36] The interatomic distances in H_2 molecules and H_3^- anions are also shown. c) Comparison of experimental powder diffraction and predicted XRD pattern of $P1\text{-CsH}_{15}$ and $Cmc\text{-CsH}$ at 22 GPa. d) Diffraction image ("cake") of CsAB decomposition products. Coarse-crystalline phase corresponds to CsH , while the disordered CsH_{15+x} phase corresponds to a series of broad diffuse diffraction lines with low intensity.

in **Figure 3**. This time, in addition to monohydride CsH ("dotted" diffraction lines, **Figure 3d**), we found a series of broad diffuse diffraction lines corresponding to the new compound with a rather large unit cell volume. Using the results of structural search in USPEX^[28-30] (**Figure 2e**; **Tables S8 and S9**, Supporting Information), we interpreted this novel compound as a non-stoichiometric molecular polyhydride $P1\text{-CsH}_{15+x}$ (where $x = -2 \dots 2$) formed by the decomposition of three or four neighboring CsAB molecules. The unit cell volume of semiconducting CsH_{15+x} is $85.3 \text{ \AA}^3/\text{Cs}$ at 22 GPa. According to the evolutionary structural search, a prototype of this phase is $P1\text{-CsH}_{17}$, located just slightly above (+3 meV atom⁻¹) the convex hull at 30 GPa. The hydrogen sublattice of CsH_{17} contains both H_2 molecules ($d_{\text{HH}} = 0.76 \text{ \AA}$) and H_3^- ions ($d_{\text{H-H}_2} = 1.35 \text{ \AA}$ at 30 GPa), which can also be considered to form van der Waals complexes (**Figure 3b**). Moreover, the latter anions were predicted earlier theoretically^[23] and found experimentally in sodium polyhydrides.^[18]

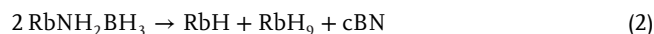
A similar series of diffuse diffraction rings can also be found in a detailed analysis of the first experiment with DAC X1. Using the information obtained from DAC X1, we established the hydrogen content in the CsH_{15+x} and the experimental unit cell volume as $\approx 100 \text{ \AA}^3/\text{Cs}$ and $x \approx 2$ at 23 GPa, although with less accuracy (**Figure 2d**).

Estimation of the hydrogen content in the synthesized CsH_{15+x} can also be approached from the other side, using the known volume of the H atom in pure hydrogen: $4.24 \text{ \AA}^3/\text{H}$ at 22 GPa.^[39] Taking the volume of Cs^+ from the equation of state of CsH_7 , we can calculate the ratio of hydrogen and cesium H: Cs in our

compound, which is between 13 and 17. Such a high hydrogen content is not surprising given the huge number of various stable and metastable solid solution compositions of Cs^+ in molecular hydrogen existing under pressure (**Figure 2e**). Similar compounds, a kind of "hydrogen sponges", can be obtained in the Sr-H ,^[7] Ba-H ,^[6] and I-H ^[40] systems at high pressure.

2.2. Synthesis of Rubidium Polyhydrides: RbH_{9-x}

Synthesis of rubidium polyhydrides was carried out starting from $\text{LT-RbAB}/\text{Rb}$ mixture (**Figure S13**, Supporting Information) via pulsed laser heating above 1000 °C at 12–12.5 GPa using a gold target in the DAC Y. The experiment was followed by decompression of the reaction products to 1.7 GPa. At pressures of 8–12 GPa, X-ray diffraction patterns of the reaction mixture (**Figure 4**) indicate the formation of a monohydride $Pm\bar{3}m\text{-RbH}$ ^[41] and two crystal modifications of rubidium polyhydride RbH_{9-x} : pseudohexagonal ($Cc\text{cm}$) and pseudotetragonal (Cm), according to the chemical reaction between two neighboring RbAB molecules:



Pseudohexagonal RbH_{9-x} is somewhat less stable from the point of view of thermodynamics and lies above the convex hull by 2.3 meV atom⁻¹ (**Figure 5c**; **Tables S6 and S7**, Supporting Information). This is an unprecedentedly low synthesis pressure for compounds of this stoichiometry. Just for the sake of

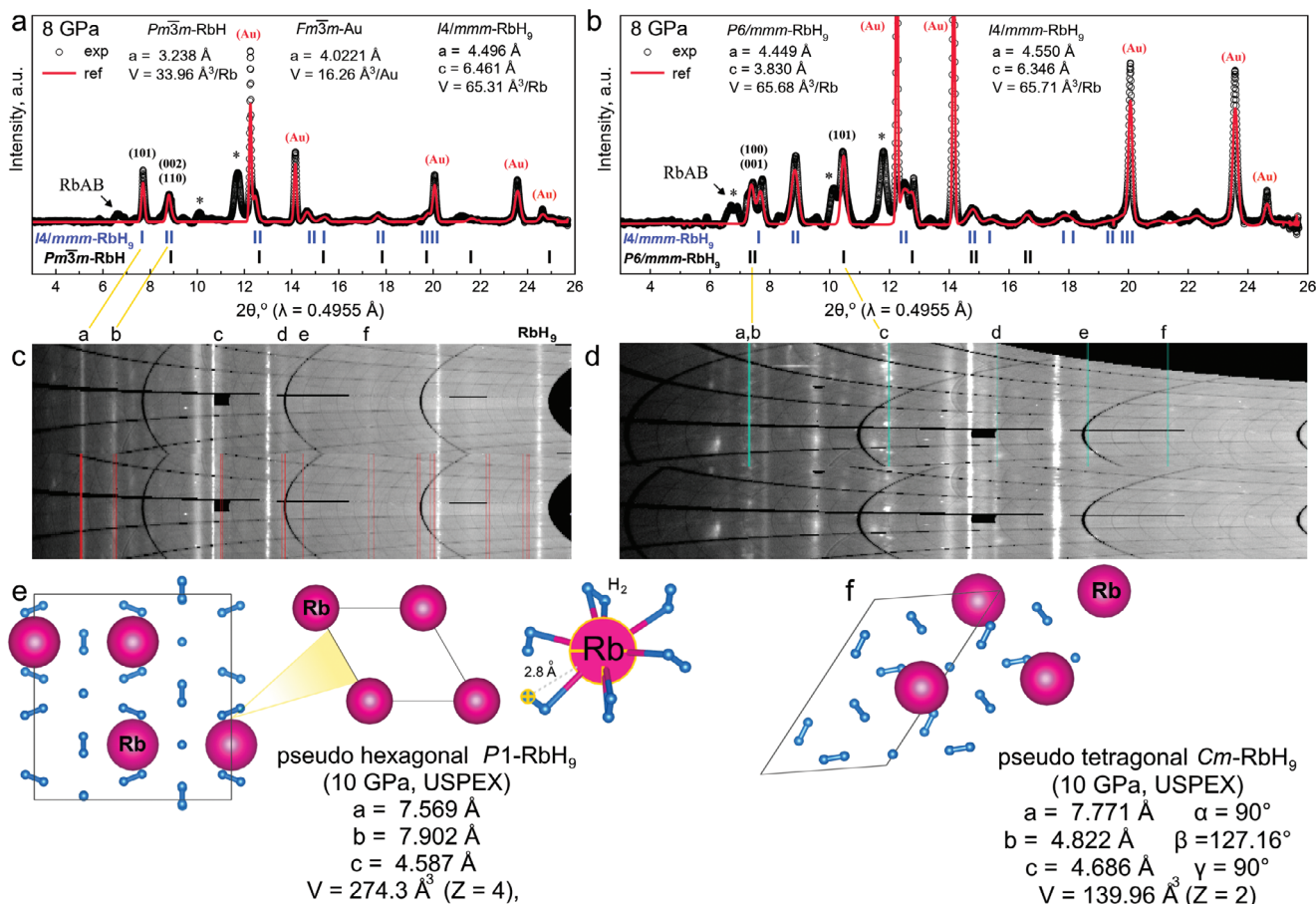


Figure 4. Formation of rubidium polyhydrides, pseudo-hexagonal, and pseudotetragonal RbH_{9-x}, from RbAB in DAC. a) Experimental X-ray diffraction pattern (black curve, λ = 0.4955 Å, and Elettra) and the Le Bail refinement (red curve) of unit cell parameters of pseudo $I4/mmm$ -RbH_{9-x} and RbH at 8 GPa. There is a broad peak of residual RbAB marked by the arrow. b) The same in another place of the sample, where there is also a pseudo $P6/mmm$ -RbH_{9-x}. Gold (Au) was used as a pressure sensor. c,d) Diffraction images (“cake”) of decomposition products of RbAB. Red and azure lines show diffraction lines (diffuse and spotted) corresponding to two structural modifications RbH_{9-x}. e,f) Crystal structure of rubidium polyhydrides obtained using USPEX^[28-30] and VASP^[34-36] codes. The calculated parameters of the unit cells of stoichiometric RbH₉, the sublattice of Rb atoms, and the coordination sphere of Rb atoms in pseudo $P6/mmm$ -RbH₉ are also given.

comparison, to obtain nonahydrides MH₉ of the neighboring elements, Sr and Y, pressures above 75–80^[42] and 200 GPa^[7,43] are required, respectively (Figure 5a,b). Comparison of experimental unit cell volumes of obtained RbH_{9-x} phases with the calculated ones (Tables S4 and S5, Supporting Information) shows that we are dealing with non-stoichiometric compounds having ≈8–9 hydrogen atoms per each rubidium atom (RbH_{9-x}, x = 0...1). A comparison with the data of Kuzovnikov et al.,^[20] who used a direct reaction of RbH with molecular hydrogen, leads to a similar conclusion.

Both obtained rubidium polyhydrides are semiconductors with wide bandgaps of ≈4.5 eV (HSE06). Molecular hydrogen sublattice in both RbH_{9-x} phases has low symmetry ($P1$), which, however, can be increased by symmetrization (tolerance is 0.2) to $Cccm$ and Cm . After that, the sublattice of rubidium atoms has a much higher space group number, $P6/mmm$ (sh) in the case of pseudo-hexagonal RbH_{9-x}, and $I4/mmm$ in the case of pseudotetragonal phase. The same is observed for BaH₁₂^[6] and SrH₉.^[7] Metal sublattice of pseudotetragonal RbH_{9-x} transforms to cubic ($Fm\bar{3}m$) after refinement, and this is one of the remarkable find-

ings of this work since this phase was not found among the products of the direct reaction of RbH with hydrogen.^[20]

Simple hexagonal ($P6/mmm$) sh-RbH₉ was recently synthesized by Kuzovnikov et al. from RbH and pure hydrogen at 24–56 GPa.^[20] This confirms the feasibility of our synthetic approach to rubidium polyhydrides starting from the corresponding amidoborane. During decompression, the authors found that sh-RbH₉ decomposes below 10 GPa. At the edge of the stability region, the volume of $P6/mmm$ -RbH₉ unit cell is ≈72 Å³/Rb,^[20] in reasonable agreement with theoretical calculations (Figure 4e, 69.3 Å³/Rb at 10 GPa). We synthesized, however, a slightly different compound with a smaller unit cell volume of V_{hex} (10 GPa) = 64.4 Å³/Rb. This speaks in favor of lower hydrogen content: RbH_{9-x} instead of RbH₉, since the volume per hydrogen atom at 10 GPa is ≈5.83 Å³/H.^[39]

It is important to note that, according to theoretical calculations of phonon spectra at 0 K, pseudotetragonal RbH₉ remains dynamically stable at ambient pressure (Figures S51–S54, Supporting Information), whereas pseudo-hexagonal RbH₉ becomes dynamically unstable below 5 GPa (Figures S48–S50,

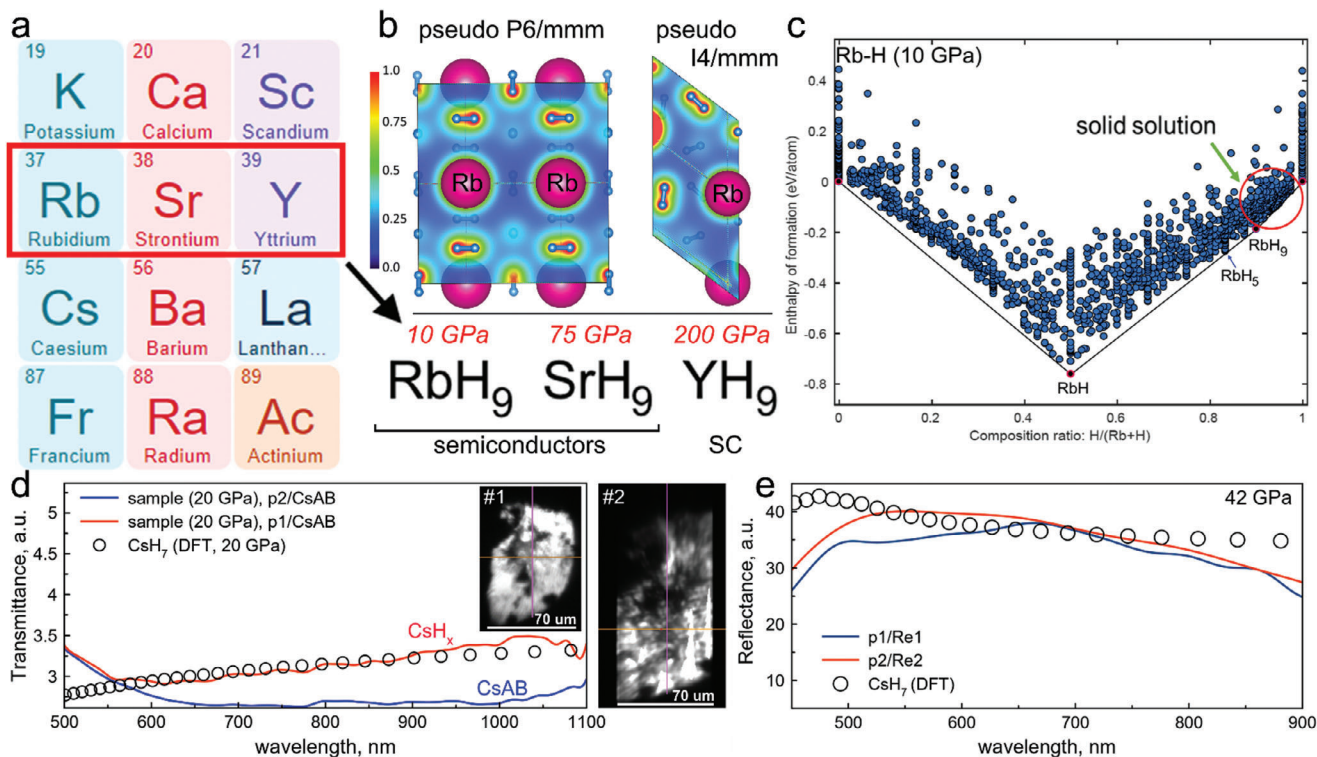


Figure 5. Physical properties and rubidium polyhydrides. a,b) A series of “isomeric” $M\text{H}_9$ polyhydrides formed by neighboring elements: Rb, Sr, and Y. The stabilization pressures of the corresponding hydrides are given in red font. “SC” means superconductor. b) Electron localization functions (ELF) of both crystal modifications of RbH_9 at 10 GPa. (100) and (010) lattice planes were used to draw ELF. Molecular hydrogen is clearly visible. c) Thermodynamic convex hull of Rb-H system at 10 GPa and 0 K calculated without ZPE. The region of solid solutions of Rb^+ cations in hydrogen is outlined in red. Stable phases at this pressure are RbH , RbH_5 , and RbH_9 . d) Experimental (“sample”) and calculated (“DFT”) relative transmittance of CsH_7 at 20 GPa compared to CsAB. Inset: photos of investigated samples, DAC X3. e) Experimental (“p1,2”) and calculated (“DFT”) relative reflectance of CsH_7 compared to the reflection from a rhenium gasket (Re1,2) at 42 GPa in DAC Z.

Supporting Information). Its experimental decomposition is observed below 8 GPa. The pseudotetragonal $\text{RbH}_{9,x}$ probably remains stable even at 3.3 GPa undergoing a structure distortion or transition. Ab initio molecular dynamics study within 10 ns at 300 K and atmospheric pressure indicates distortion of the pseudotetragonal structure of RbH_9 that is also observed experimentally. Despite the distortion of the Rb sublattice, H_2 molecules in RbH_9 oscillate near equilibrium positions, and have no pronounced diffusion tendency.

2.3. Raman Spectroscopy

Raman spectra of cesium hydrides was studied at room temperature at excitation laser wavelengths of 532 and 633 nm. Before the laser heating, samples of amidoboranes in DACs exhibit a set of Raman signals consistent with the literature data for RbAB and CsAB (Figures S9, S10, and S13, Supporting Information). After laser heating of CsAB, a new broad peak appears at 3850 cm^{-1} (at 18–21 GPa, Figure S11, Supporting Information). According to the results of ab initio calculations, this broad peak should be assigned to $P4/nmm\text{-CsH}_7$ (Figure S12, Supporting Information). A double peak of molecular hydrogen was detected near the vibration frequency of pure H_2 (Figure S11, Supporting Information). At the same time, in experiments with LiAB and NaAB, a

similar Raman peaks were detected between 2900 and 3800 cm^{-1} possibly indicating the formation of Li and Na polyhydrides (Figures S7 and S8, Supporting Information).

The situation for rubidium polyhydrides is similar. Raman spectrum of RbAB/Au after laser heating has a broad peak at $3800\text{--}3900\text{ cm}^{-1}$ (Figures S14 and S15, Supporting Information), which corresponds to $\text{RbH}_{9,x}$ in agreement with the results of direct synthesis of $P6/mmm\text{-RbH}_9$ from RbH and H_2 ^[20] and ab initio calculations (Figure S16, Supporting Information). In addition, there is a peak of molecular hydrogen (4242 cm^{-1}). Thus, for cesium and rubidium polyhydrides, Raman spectroscopy confirms the formation of molecular hydrogen, CsH , CsH_7 , and $\text{RbH}_{9,x}$, although the spectra contain other peaks that are difficult to interpret.

2.4. Reflectance and Transmittance Spectroscopy

We investigated the relative reflectance $R(\lambda)$ of Cs and CsAB before and after laser heating in the high-pressure DAC X3 at 42 GPa and in DAC Z at 20 GPa in the visible spectral range (400–900 nm, 1.4–3.1 eV). Because the precise geometry of stressed diamond anvils, Cs particle, and CsNH_2BH_3 layer is not completely known, it is only possible to determine the relative reflectance or transmittance of samples in comparison with the

reflection/transmission from either the rhenium (Re) gasket or an “empty” place, such as the diamond/CsNH₂BH₃ (or AB) boundary. The relative reflectance and transmittance were calculated as $R(\lambda)$ or $T(\lambda) = \text{const} \times I_{\text{sample}}(\lambda)/I_{\text{ref}}(\lambda)$, where $I_{\text{sample}}(\lambda)$ and $I_{\text{ref}}(\lambda)$ are intensities of light reflected from or transmitted through the sample and the reference point, respectively. Reflectance spectra of the compressed technetium hydride TcH_{1.3} were recently measured and processed in the same way.^[44,45]

Surprisingly, transmission measurements of a thin Cs particle at 42 GPa result in a $T(\lambda)$ similar to the literature data at 0 GPa (Figure S20, Supporting Information). After the laser heating of Cs/CsAB, an almost transparent substance (e.g., CsH_x) is formed, which makes optical research challenging and the results – qualitative. When using the transmittance of CsAB as a reference, we found good agreement between the calculated transmittance of CsH₇ and the experimental data obtained after laser heating of Cs/CsAB (Figure 5d). At the same time, the difference between CsAB and CsH_x is insignificant when using an empty DAC as a reference.

Reflectivity of Cs at 20 GPa is also in good agreement with the literature data (Figure S19, Supporting Information). Laser heating of the Cs/CsAB sample at 42 GPa, as expected, leads to a significant drop in the sample reflectivity (compared to Cs), a change in the sign of $dR/d\lambda$ and a monotonic decrease in $R(\lambda)$ in the range of 500–950 nm (Figure 5e). This behavior is in qualitative agreement with the results of DFT calculations for CsH₇ (Figure S23, Supporting Information). Therefore, optical spectroscopy confirms the formation of CsH₇ during the thermal decomposition of cesium amidoborane.

3. Discussion

3.1. Structural Features of Cs and Rb Polyhydrides

Proposed method for the synthesis of polyhydrides by heating their amidoboranes under pressure opens up prospects for obtaining not only Cs and Rb polyhydrides but also polyhydrides of all alkaline and alkaline-earth metals, as well as Y and Zn. Encouraging results from trial experiments with LiAB, NaAB, and Ca(AB)₂ are given in the Supporting Information. The proposed approach affects not only binary but also ternary polyhydrides. Indeed, by crystallizing solutions of different amidoboranes from organic solvents, it is easy to obtain mixed amidoboranes. Many of them have been previously described experimentally.^[46] Their thermal decomposition under pressure will lead to formation of ternary polyhydrides of Li-Na, Na-Mg, etc.

Discovery of ultrastable cesium and rubidium polyhydrides raises the question of the possibility of further increasing stability of H-rich compounds at ambient conditions. Promising is the design of such compounds using larger ions, atoms, and molecules (“pseudo atoms”) such as Xe,^[47] (CH₃)₃N⁺ and tert-butylammonium cation (*t*-Bu)₃N⁺, methane molecule,^[48] neopentane C(CH₃)₄, and various halogen-substituted molecules: CF₄, SF₆, Cl₄ and so on.

During this study, we noticed one fascinating analogy between the structure of higher metal polyhydrides and the physics of space plasma. Properties of many polyhydrides of alkali and alkaline earth metals are similar to the behavior of plasma crystals, in which heavy dust grains (say, Rb⁺, Sr⁺², etc.) are surrounded by a

Debye cloud of much smaller ions (e.g., H⁻, H₃⁻) with an opposite charge. In this case, heavy atoms usually form a highly symmetric sublattice. This is an effect, well-known from the study of plasma crystals in microgravity.^[49] Structures of RbH_{9,x}, CsH_{15+x}, and SrH₂₂, are kind of plasma crystals because a large charged metal ion (Cs⁺, Rb⁺) has a Debye shell of weakly charged light (H_{2±1})⁻ anions around. In the space, these spherical shells are organized into a cubic or hexagonal close packings, where metal atoms become a kind of raisins in a pie made of hydrogen (Figure S60, Supporting Information).

Tendency to form such solid electrolytes from Cs⁺ and Rb⁺ ions dissolved in molecular hydrogen already follows from thermodynamic calculations of Cs-H and Rb-H convex hulls, where the entire region near pure hydrogen is filled with higher polyhydrides even at low pressures (Figure 2e and Figure 5c). These polyhydrides are stabilized by the electric field of cesium and rubidium ions separated via a mobile shell of hydrogen. As it has been shown in experiments with BaH₂,^[37] SrH_{5.75},^[7] and by molecular dynamics simulations of H₃Cl^[38] and LaH₁₀,^[50,51] hydrogen in such polyhydrides has very high diffusivity causing significant ionic conductivity and even superionicity, probably exceeding that of BaH₂.^[37]

4. Conclusion

To sum up, using synchrotron X-ray powder diffraction, Raman spectroscopy, optical measurements, and first-principles calculations, we demonstrated that Cs and Rb amidoboranes can be used to synthesize corresponding molecular polyhydrides: *P4/nmm*-CsH₇, CsH_{15+x} and two crystal modifications of RbH_{9,x}. Our proposed approach to polyhydrides from readily available amidoboranes does not require the use of hydrogen loading systems and can be extended to binary and ternary polyhydrides of other alkali (Li and Na) and alkaline earth (Ca) metals. We observed amorphization of Cs and Rb amidoboranes above 20–30 GPa. As a result, they practically do not contribute to the diffraction patterns of Cs and Rb polyhydrides.

All synthesized Cs and Rb polyhydrides are ultrastable molecular-ionic semiconductors with a bandgap of 2.6–4.5 eV. Compared to many other hydrides, Cs and Rb require external pressure of only 10–20 GPa, instead of 100–200 GPa for La, Y, Ba, Ce, Th, and other metal polyhydrides. During decompression, CsH₇ may remain stable until the pressure in DAC is almost completely released. Exploring the thermodynamics of hydride synthesis, we found that cesium and rubidium tend to form nonstoichiometric compounds with an excess of hydrogen under pressure. Large Rb⁺ and Cs⁺ ions locate in the disordered lattice of molecular hydrogen. Adding or removing one H₂ molecule from such a hydrogen “pie” has virtually no effect on the enthalpy of formation of hydrogen-rich compounds. Considering the molecular-ionic nature of the Cs and Rb hydrides, high diffusivity of hydrogen already at room temperature, as well as the low symmetry of the hydrogen sublattice, all the resulting compounds will likely exhibit pronounced ionic conductivity.

Our work demonstrates that cesium and rubidium have prospects for increasing the capacity of hydrogen batteries by stabilizing the shell of molecular hydrogen, and open a way for further reducing the synthesis pressure of polyhydrides.

Supporting Information

Supporting Information is available from the Wiley Online Library or from the author.

Acknowledgements

D.S. and D.Z. thank the National Natural Science Foundation of China (NSFC, grant No. 1231101238) and the Beijing Natural Science Foundation (grant No. IS23017) for support of this research. D.Z. thanks the China Postdoctoral Science Foundation (Certificate No. 2023M740204) and financial support from HPSTAR. This work was partially supported by JSPS KAKENHI Grant Number 20H05644. The high-pressure experiments were supported by the Russian Science Foundation (Project No. 22-12-00163). The authors also thank the Center for Energy Science and Technology, the Center for Photonic Science and Engineering, and the Center for Engineering Physics of Skoltech for the opportunity to use the center's equipment during the implementation of this project. A.R.O. thanks the Russian Science Foundation for supporting his work (grant 19-72-30043). All authors thank the staff scientists of the SPring-8 and Elettra (proposals No. 20215034 and No. 20220288) synchrotron radiation facilities for their help with X-ray diffraction measurements, especially Dr. Saori Kawaguchi (SPring-8) and Dr. Boby Joseph (Elettra). This work was started at Jilin University in 2019 with the support of Prof. Xiaoli Huang. The authors express their gratitude to Dr. Mikhail Kuzovnikov (University of Edinburgh) and Dr. Vadim Efimchenko (IPSS RAS, Chernogolovka) for providing CsH samples and valuable discussions. The authors thank Dr. Pavel Zinin (STC UI RAS, Moscow) for assistance in laser heating.

Conflict of Interest

The authors declare no conflict of interest.

Author Contributions

D.Z. and D.S. contributed equally to this work. D.Z., D.S., M.G., F.G.A., I.T., Y.N., and K.S. performed experiments. D.Z., M.G., and D.S. prepared the theoretical part of the paper. D.Z., D.S., and A.R.O. analyzed the data and wrote the paper. All the authors discussed the results and offered useful inputs.

Data Availability Statement

The data that support the findings of this study are available from the corresponding author upon reasonable request.

Keywords

amidoboranes, cesium hydride, high pressure, polyhydrides, rubidium hydride

Received: January 5, 2024

Revised: March 20, 2024

Published online:

- [1] N. A. A. Rusman, M. Dahari, *Int. J. Hydrogen Energy* **2016**, *41*, 12108.
[2] M. Marshall, Z. Zhu, R. Harris, K. H. Bowen, W. Wang, J. Wang, C. Gong, X. Zhang, *Chemphyschem* **2021**, *22*, 5.

- [3] S. J. Huang, H. Y. Wang, S. M. Li, G. Z. Zhang, Y. Su, *Int. J. Hydrogen Energy* **2022**, *47*, 420.
[4] I. A. Troyan, D. V. Semenok, A. G. Kvashnin, A. V. Sadakov, O. A. Sobolevskiy, V. M. Pudalov, A. G. Ivanova, V. B. Prakapenka, E. Greenberg, A. G. Gavriluk, I. S. Lyubutin, V. V. Struzhkin, A. Bergara, I. Errea, R. Bianco, M. Calandra, F. Mauri, L. Monacelli, R. Akashi, A. R. Oganov, *Adv. Mater.* **2021**, *33*, 2006832.
[5] W. Chen, D. V. Semenok, X. Huang, H. Shu, X. Li, D. Duan, T. Cui, A. R. Oganov, *Phys. Rev. Lett.* **2021**, *127*, 117001.
[6] W. Chen, D. V. Semenok, A. G. Kvashnin, X. Huang, I. A. Kruglov, M. Galasso, H. Song, D. Duan, A. F. Goncharov, V. B. Prakapenka, A. R. Oganov, T. Cui, *Nat. Commun.* **2021**, *12*, 273.
[7] D. V. Semenok, W. Chen, X. Huang, Di Zhou, I. A. Kruglov, A. B. Mazitov, M. Galasso, C. Tarrantini, X. Gonze, A. G. Kvashnin, A. R. Oganov, T. Cui, *Adv. Mater.* **2022**, *34*, 2200924.
[8] X. Wang, L. Andrews, I. Infante, L. Gagliardi, *J. Am. Chem. Soc.* **2008**, *130*, 1972.
[9] X. Wang, L. Andrews, *J. Phys. Chem. A* **2011**, *115*, 14175.
[10] X. Wang, L. Andrews, I. Infante, L. Gagliardi, *J. Phys. Chem. A* **2009**, *113*, 12566.
[11] X. Wang, L. Andrews, *Organometallics* **2008**, *27*, 4273.
[12] X. Wang, L. Andrews, L. Gagliardi, *J. Phys. Chem. A* **2008**, *112*, 1754.
[13] J. Raab, R. H. Lindh, X. Wang, L. Andrews, L. Gagliardi, *J. Phys. Chem. A* **2007**, *111*, 6383.
[14] J. G. Hinman, A. J. Lough, R. H. Morris, *Inorg. Chem.* **2007**, *46*, 4392.
[15] I. A. Troyan, D. V. Semenok, A. G. Ivanova, A. G. Kvashnin, D. Zhou, A. V. Sadakov, O. A. Sobolevsky, V. M. Pudalov, A. R. Oganov, *Phys.-Usp.* **2022**, *65*, 748.
[16] C. Pépin, P. Loubeyre, F. Occelli, P. Duma, *Proc. Natl. Acad. Sci. USA* **2015**, *112*, 7673.
[17] T. Matsuoka, K. Kuno, K. Ohta, M. Sakata, Y. Nakamoto, N. Hirao, Y. Ohishi, K. Shimizu, T. Kume, S. Sasaki, *J. Raman Spectrosc.* **2017**, *48*, 1222.
[18] V. V. Struzhkin, D. Y. Kim, E. Stavrou, T. Muramatsu, H. K. Mao, C. J. Pickard, R. J. Needs, V. B. Prakapenka, A. F. Goncharov, *Nat. Commun.* **2016**, *7*, 12267.
[19] T. Marqueño, M. A. Kuzovnikov, I. Osmond, P. Dalladay-Simpson, A. Hermann, R. T. Howie, M. Peña-Alvarez, *Front Chem.* **2024**, *11*, 1306495.
[20] M. Kuzovnikov, Synthesis of novel rubidium superhydrides under high-pressure in 28th AIRAPT and 60th EH-PRG International Conference, Edinburgh, **2023**, <https://az659834.vo.msecnd.net/eventsairwesteuprod/production-iop-public/6f1b25d61ee04e1090f5e71352cb88c0>.
[21] J. Kim, Oral report in 10th Asian Conference on High-Pressure Research, Hanyang University, Busan, **2021**.
[22] A. Shamp, J. Hooper, E. Zurek, *Inorg. Chem.* **2012**, *51*, 9333.
[23] J. Hooper, E. Zurek, *Chem. - Eur. J.* **2012**, *18*, 5013.
[24] M. J. Hutcheon, A. M. Shipley, R. J. Needs, *Phys. Rev. B* **2020**, *101*, 144505.
[25] J. Hooper, P. Baettig, E. Zurek, *J. Appl. Phys.* **2012**, *111*, 112611.
[26] R. Owarzany, T. Jaroń, P. J. Leszczyński, K. J. Fijalkowski, W. Grochala, *Dalton Trans.* **2017**, *46*, 16315.
[27] S. Dmitrii, CsHx heating 35–40GPa, https://www.youtube.com/watch?v=R2MG0XMX_K4, **2021**.
[28] C. W. Glass, A. R. Oganov, N. Hansen, *Comput. Phys. Commun.* **2006**, *175*, 713.
[29] A. R. Oganov, C. W. Glass, *J. Chem. Phys.* **2006**, *124*, 244704.
[30] A. O. Lyakhov, A. R. Oganov, H. T. Stokes, Q. Zhu, *Comput. Phys. Commun.* **2013**, *184*, 1172.
[31] K. Ghandehari, H. Luo, A. L. Ruoff, S. S. Trail, F. J. DiSalvo, *Phys. Rev. Lett.* **1995**, *74*, 2264.
[32] A. Le-Bail, *Powder Diffr.* **2005**, *20*, 316.

- [33] C. F. Macrae, I. Sovago, S. J. Cottrell, P. T. A. Galek, P. McCabe, E. Pidcock, M. Platings, G. P. Shields, J. S. Stevens, M. Towler, P. A. Wood, *J. Appl. Crystallogr.* **2020**, *53*, 226.
- [34] G. Kresse, J. Furthmüller, *Phys. Rev. B* **1996**, *54*, 11169.
- [35] G. Kresse, J. Hafner, *Phys. Rev. B* **1994**, *49*, 14251.
- [36] G. Kresse, J. Hafner, *Phys. Rev. B* **1993**, *47*, 558.
- [37] M. C. Verbraeken, C. Cheung, E. Suard, J. T. S. Irvine, *Nat. Mater.* **2015**, *14*, 95.
- [38] J. Binns, A. Hermann, M. Peña-Alvarez, M.-E. Donnelly, M. Wang, I. Kawaguchi Saori, E. Gregoryanz, T. Howie Ross, P. Dalladay-Simpson, *Sci. Adv.* **2021**, *7*, eabi9507.
- [39] P. Loubeyre, R. LeToullec, D. Hausermann, M. Hanfland, R. J. Hemley, H. K. Mao, L. W. Finger, *Nature* **1996**, *383*, 702.
- [40] J. Binns, P. Dalladay-Simpson, M. Wang, G. J. Ackland, E. Gregoryanz, R. T. Howie, *Phys. Rev. B* **2018**, *97*, 024111.
- [41] F. A. Lewis, A. Aladjem, *Hydrogen Metal Systems I*, Trans Tech Publications Ltd., Switzerland **1996**, 474.
- [42] P. Kong, V. S. Minkov, M. A. Kuzovnikov, A. P. Drozdov, S. P. Besedin, S. Mozaffari, L. Balicas, F. F. Balakirev, V. B. Prakapenka, S. Chariton, D. A. Knyazev, E. Greenberg, M. I. Eremets, *Nat. Commun.* **2021**, *12*, 5075.
- [43] M. Peña-Alvarez, J. Binns, M. Marqués, M. A. Kuzovnikov, P. Dalladay-Simpson, C. J. Pickard, G. J. Ackland, E. Gregoryanz, R. T. Howie, *J. Phys. Chem. Lett.* **2022**, *13*, 8447.
- [44] F. Capitani, B. Langerome, J. B. Brubach, P. Roy, A. Drozdov, M. I. Eremets, E. J. Nicol, J. P. Carbotte, T. Timusk, *Nat. Phys.* **2017**, *13*, 859.
- [45] P. Roy, J. B. Brubach, F. Capitani, B. Langerome, A. Drozdov, M. I. Eremets, E. J. Nicol, T. Timusk, *Nat. Phys.* **2022**, *18*, 1036.
- [46] R. Owarzany, P. J. Leszczyski, K. J. Fijalkowski, W. Grochala, *Crystals* **2016**, *6*, 88.
- [47] M. Somayazulu, P. Dera, A. F. Goncharov, S. A. Gramsch, P. Liermann, W. Yang, Z. Liu, H.-k. Mao, R. J. Hemley, *Nat. Chem.* **2010**, *2*, 50.
- [48] U. Ranieri, L. J. Conway, M.-E. Donnelly, H. Hu, M. Wang, P. Dalladay-Simpson, M. Peña-Alvarez, E. Gregoryanz, A. Hermann, R. T. Howie, *Phys. Rev. Lett.* **2022**, *128*, 215702.
- [49] V. E. Fortov, A. G. Khrapak, S. A. Khrapak, V. I. Molotkov, O. F. Petrov, *Phys.-Usp.* **2004**, *47*, 447.
- [50] X. Qin, H. Wu, G. Shi, C. Zhang, P. Jiang, Z. Zhong, *Phys. Rev. B* **2023**, *108*, 064102.
- [51] M. Caussé, G. Geneste, P. Loubeyre, *Phys. Rev. B* **2023**, *107*, L060301.